

# Super-Resolution Perception for Industrial Sensor Data

Jinjin Gu, Guolong Liu, Gaoqi Liang, Junhua Zhao

School of Science and Engineering, The Chinese University of Hong Kong, Shenzhen  
{115010148, 216019006}@link.cuhk.edu.cn, {lianggaoqi, zhaojunhua}@cuhk.edu.cn

## Abstract

In this paper, we present the problem formulation and methodology framework of Super-Resolution Perception (SRP) on industrial sensor data. Industrial intelligence relies on high-quality industrial sensor data for system control, diagnosis, fault detection, identification and monitoring. However, the provision of high-quality data may be expensive in some cases. In this paper, we propose a novel machine learning problem - the SRP problem as reconstructing high-quality data from unsatisfactory sensor data in industrial systems. Advanced generative models are then proposed to solve the SRP problem. This technology makes it possible for empowering existing industrial facilities without upgrading existing sensors or deploying additional sensors. We first mathematically formulate the SRP problem under the Maximum a Posteriori (MAP) estimation framework. A case study is then presented, which performs SRP on smart meter data. A network namely SRPNet is proposed to generate high-frequency load data from low-frequency data. Experiments demonstrate that our SRP model can reconstruct high-frequency data effectively. Moreover, the reconstructed high-frequency data can lead to better appliance monitoring results without changing the monitoring appliances.

## Introduction

Industry is a vital part of the economy that produces commodities in a centralized, mechanized and automatized way. With the introduction of Industry 4.0, a new fundamental paradigm shift in industrial production is resulted by the combination of Internet technologies and emerging technologies in the field of smart objects (machines and products) (Lasi et al. 2014). The rapid development of industrial intelligence will bring tremendous impact on various fields of the society.

Industrial intelligence is a key driver of the 4th Industrial Revolution, which can enable precise sensing and control of industrial systems through a large number of industrial sensors (Abramovici, Göbel, and Neges 2015). In the modern industry, in order to improve the operating efficiency and product quality, higher accuracy of sensing and control are essential. This will lead to higher dependency on high precision and resolution data.

Collecting high-resolution state data of an industrial system is essential because of the following reasons. Firstly, many industrial systems, such as aero engines, chemical

processes, manufacturing systems, and power networks are safety-critical systems. Reliability and safety are of utmost importance to these industrial systems, which however are vulnerable to potential process abnormalities and component faults (Gao, Cecati, and Ding 2015). Their tolerance to abnormality is very small, once small errors or abnormal fluctuations may cause serious consequences or losses. In practice, low-resolution state data may not be sufficient for detecting or rectifying system anomalies or faults. This may lead to permanent system damage or other potential security risks. For instance, a 1Hz frequency meter cannot measure the current overload that lasts less than 1s, the over-current event not detected by the low-frequency meters will lead to premature aging of the equipment and cause inestimable security risks. The inherent defects of low-frequency meters limit the capability of an industrial system to perceive and control its internal states in a more precise manner.

Secondly, accurate state monitoring is the basis for optimization and control of an industrial system. In practice, the frequency of control actions is limited by the sampling frequency of meters. If the time interval between two control actions is too large, the economic efficiency or security of the system may be compromised. Take wind turbine as an example, the parameters of a wind turbine (e.g. blade angle) must be optimized according to the varying wind speed to increase the wind power output. If the time interval between two wind speed measurements is 5 minutes, it then means the wind power output of this turbine is not optimized within these 5 minutes. This is because the wind speed is constantly varying, the wind turbine is therefore not working in its optimal state.

In principle, installing higher-resolution meters is an ideal solution to the above problems. However high-resolution meters have higher costs as well. On the other hand, this also means that a large number of low-resolution meters installed before have to be replaced, which is a huge waste of resources for large systems like power grids. Therefore, in this paper, we propose a novel machine learning problem namely Super Resolution Perception (SRP). The proposed SRP problem aims at recovering high-resolution system state data from low-resolution data collected by the existing low-resolution meters, which can then be used to support more accurate and reliable state monitoring, optimization and control.

There are at least four types of problems that can be solved by employing SRP. Firstly, without using high-resolution meters, SRP can support the high-resolution state monitoring of industrial systems. In practical industrial systems, sensors with different sampling frequencies may co-exist, which cannot satisfy the data quality requirement of precise control. By converting low-resolution data to higher resolution data, SRP provides a novel and practical way to solve this problem.

Secondly, the problem of bad data and data losses can also be improved by using SRP. It is very common that bad data are generated in some special cases during the operation of industrial systems, or the measurement data are lost during transmission. Although state estimation and bad data detection, which are important components in industrial systems, can identify and eliminate bad data (Bretas, Bretas, and Martins 2013), the removed data cannot not be supplemented which therefore influences the accuracy of estimated system statuses. Through the detailed information provided by SRP, the bad data and missing data can not only be detected but also be well recovered, which contributes to any component that is operated based on collected data.

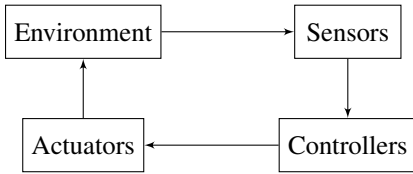


Figure 1: Flowchart of general control process.

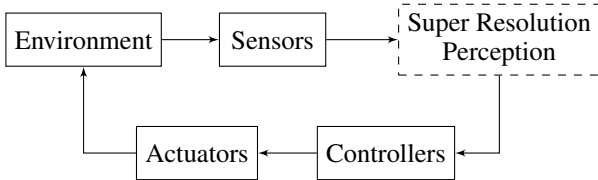


Figure 2: Flowchart of control process with SRP.

Thirdly, security constrained operation is vital for safety-critical industrial systems. In practice, every industry system must work in its specific security region, e.g. the temperature of a boiler must be maintained within a reasonable range. However, when the industrial sensors have insufficient sampling frequency, quality and security variables will be difficult to measure (Qin 2012). This will lead to the risk that the system works in an unsafe state temporarily, which will compromise the lifetime and reliability of the system. The high-resolution data produced by SRP can help precisely control the state variables within the security regions and thus mitigate this kind of risks.

At last, high-precision control strategies require high-resolution data. The general flowchart of a control process is shown in Figure 1. Traditional industrial control sys-

tems (ICS) are based on mechanical or electrotechnical devices and closed systems. Today, these systems have become more expensive to deploy, maintain and operate due to the higher functional requirements of modern industry. To address these challenges, more communication devices and sensors are being integrated into these systems, which in turn makes the systems more complex at the hardware level (Kriaa et al. 2015). Different from relying on high-resolution sensors, SRP can reproduce high-resolution state data from low-resolution sensors and support the high-precision control (shown in Figure 2). This comes with almost no increase in system complexity and additional investments on sensors and communications.

In summary, this paper introduces a novel machine learning problem called Super Resolution Perception, to recover high-resolution industrial sensor data from low-resolution data. Our main contributions in this paper are:

- We are among the first to put forward the problem of SRP for industrial sensor data. Specifically, we propose a framework based on low-frequency sampling data to have a more precise perception of industrial systems.
- The method of applying deep learning to solve temporal dimension SRP namely SRPNet is proposed for the first time. Considering the security problems, such as power overload in industrial systems, this paper proposes a new feasible method to ensure the security of the system.
- This paper has proved the value and effectiveness of SRP using smart meter data as a case study. Based on the high-resolution data produced by SRP, better control strategies and control effects can be achieved for smart grids.

## Related Work

As the machine learning tool for solving SRP, deep generative models are introduced in this section. Different from discriminative models that try to infer the conditional probability of the label when data is given, generative models directly infer the probability distribution of data. Due to the powerful approximation ability of deep neural networks, deep learning based generative models have been widely used for data generation and processing. Some advanced generative models have been very successful in generating images from noise vectors (Kingma and Welling 2014; Rezende, Mohamed, and Wierstra 2014; Goodfellow et al. 2014). Other deep generative models are also widely used for image processing, such as image denoising (Mao, Shen, and Yang 2016; Zhang et al. 2017b), deblurring (Kupyn et al. 2017; Zhang et al. 2017a) and inpainting (Yeh et al. 2017). Moreover, specialized generative models are used to generate time series. Van Den Oord et al. (Van Den Oord et al. 2016) use dilated causal convolutional neural network to generate high temporal resolution raw audio waveforms (more than 16000 samples per second) and it shows strong results in generating voices and other audio modalities such as music. More relevant to the proposed SRP problem, deep generative models are also used in single image super-resolution (SISR). SISR aims at recovering a high-resolution image from a single low-resolution one. Dong et al. (Dong

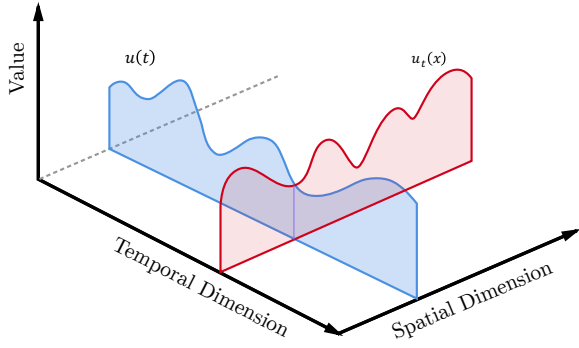


Figure 3: The relationship of temporal dimension and spatial dimension. When  $u(t)$  is a scalar,  $u$  is a function of time  $t$ . When  $u(t) = u_t(x)$  is a function of  $x$  in spatial dimension,  $u$  can be viewed as a multivariable function of  $t$  and  $x$ .

et al. 2016) first train a three layer convolutional neural network (CNN) for image super-resolution. Some works (Kim, Lee, and Lee 2016; Lim et al. 2017) then use very deep CNN for better reconstruction results. Although SISR based on deep learning has been very effective in passed a few years. However, to the best of our knowledge, there is no suitable way to super-resolve non-image signals such as time series waveform data.

### Problem Formulation

Consider a continuous-space physical quantity  $u$ . The value of  $u$  at time  $t$  can be denoted by  $u(t)$ . Let  $l$  denote a low-resolution sensor data and  $h$  denote the high-resolution sensor data of same physical quantity. The low-res data is generated from  $u$  by a continuous sampling function  $\delta_L$  and the value of  $l$  at time period  $[t_{start}, t_{end}]$  can be wrote as

$$l[t_n] = \int u(t)\delta_L(t - t_n)dt + n, t_n \in [t_{start}, t_{end}]$$

where  $n$  is noise. The high-res data  $h$  of same time period but with a finer grid is as

$$h[t_m] = \int u(t)\delta_H(t - t_m)dt + n, t_m \in [t_{start}, t_{end}]$$

where  $\delta_H$  denote high-resolution sampling function and the time index  $t_m$  of  $h$  is more dense. Note that at same time  $t_0$ ,  $h[t_0]$  and  $l[t_0]$  may not equal because of the difference of  $\delta_H$  and  $\delta_L$ . Both  $l$  and  $h$  represent the value of the same physical quantity in the same time period, but  $h$  contains richer information on describing  $u$ .  $h$  and  $l$  are related by a degradation model:

$$l = \downarrow h + n$$

where  $\downarrow$  is the degradation function and  $n$  is noise. SRP can be viewed as trying to inference  $h$  with  $l$  as input. SRP aims to find a reconstruction mapping  $f$  that the reconstructed high-res data  $h' = f(l)$  that recovers the information lost by degradation function as much as possible.

The purpose of SRP is different depending on the property of  $u$  and degradation function  $\downarrow$ . If the loss of

information caused by degradation function is reflected in frequency reduction in the temporal dimension, the problem of restoring such temporal information is called *Temporal SRP* problem. According to different application scenarios,  $u(t)$  can be a scalar or a function on spatial dimension  $u(t) = u_t(x)$ , where  $x$  denote the spatial position. If the degradation process loses the spatial information, the corresponding SRP problem is called *Spatial SRP* problem. The SRP problem considering both temporal and spatial dimension is called *Spatial-Temporal SRP* problem. The relationship between temporal and spatial dimension is shown by Figure 3. For different kind of degradation functions, SRP problem can be viewed as a superset of the various data quality problems, such as incomplete data, bad data and malicious data, etc.

### Interpretation of SRP as MAP estimation

We next show that the SRP can be viewed as Maximum a Posteriori (MAP) estimation. For a given low-res sensor data  $l$ , there are many possible  $h$  satisfying the degradation function. The final estimated  $h$  is the solution with maximum posterior probability  $p(h|l)$ . According to the Bayesian formula, the posterior probability can be written as

$$p(h|l) = \frac{p(l|h)p(h)}{p(l)}$$

where  $p(l|h)$  is the likelihood,  $p(h)$  is the prior on  $h$  and  $p(l)$  is a constant when  $l$  is given. The corresponding  $h$  given a specific  $l$  can be estimated by solving the MAP problem

$$h' = \arg \max_h p(h|l) = \arg \max_h p(l|h)p(h)$$

which is equivalent to solving the following formula

$$h' = \arg \max_h \log p(l|h) + \log p(h)$$

in which  $p(l|h)$  can be solved by modeling the degradation process and  $p(h)$  is obtained by solving the prior model. This indicates that the  $h$  estimated by the SRP should not only satisfy the degradation model but also satisfy the priori characteristics of  $h$ . The prior term  $p(h)$  can be viewed as regularization term. Effectively modeling the prior of  $h$  is important to SRP problems.

### Case Study

In this paper, we study the SRP problem using smart meter data as an example. Smart meter data is collected by a single measurement unit (meter) and it records the overall electricity consumption of a household. This data can be used for monitoring, analysis and identification of load. The frequency of the meter data depends on the sampling frequency of the smart meter. High-frequency meter data contains more information and can be better used for monitoring and analysis of electricity consumption. However, existing measurement units are mostly low-frequency units, which cannot produce high-frequency observation data directly. We use SRP to process low-frequency load data and re-produce possible high-frequency data with an end-to-end

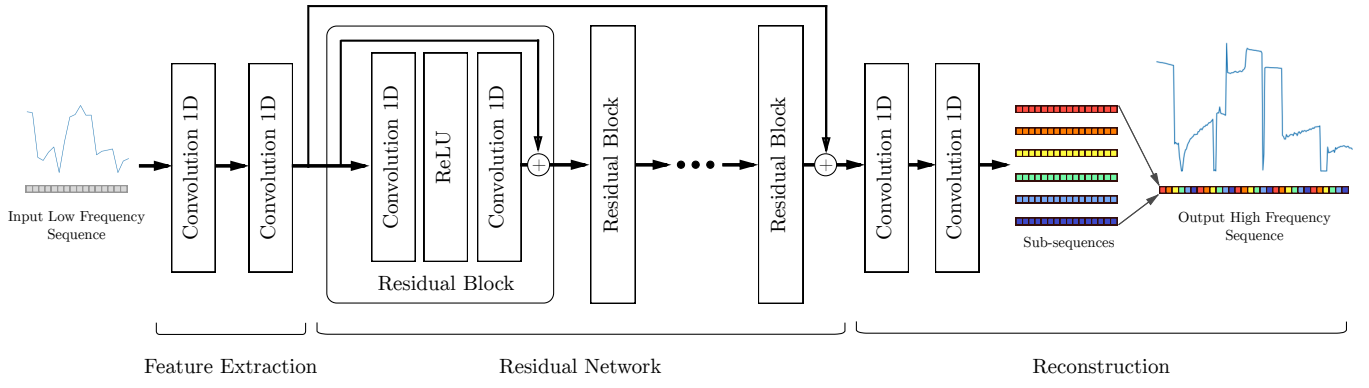


Figure 4: The proposed Super-resolution Preception Network (SRPNet). with two convolution layers for feature maps extraction, and a sub-pixel convolution layer that aggregates the feature maps from LR space and builds the SR image in a single step.

neural network SRPNet. We further prove that the use of estimated high-frequency data can lead to better appliance monitoring results without changing monitoring method. In this case, the physical quantity  $u(t)$  represents the instantaneous power at time  $t$ , which is a scalar. The load data in a certain period of time appears as a sequence.

## Method

For a given time period, we denote the low-res load data collected by low frequency meters as  $x$  with frequency  $f_l$ . The corresponding high-re data is  $y$  and with a higher frequency  $f_h$ . For a single meter,  $x(t)$  is a scalar and  $x \in \mathbb{R}^d$ ,  $d$  denote the length of low-res data. With a super-resolution factor  $\alpha$ , we have  $f_h = \alpha f_l$  and thus  $y \in \mathbb{R}^{\alpha d}$ . According to the degradation model, we have  $y = \downarrow x + n$ . Our goal is to recover  $y$  from  $x$  by a SRP mapping  $f$ . We use a deep convolutional neural network called SRPNet to implement the mapping.

The network architecture of SRPNet is shown in Figure 4. SRPNet takes the low-frequency data as the input and outputs the estimated high-frequency data directly. At top of the network, two 1D convolution layers are operated as a global feature extractor. This extractor extracts features from low-res input and represents the features as many feature vectors. These vectors contain the abstract feature information of input and each vector has the same dimension with as input data. After feature extraction, an information supplemental sub-network with the residual structure is used to supplement the lost information to the feature vectors. The residual structure consists of a big global residual connection and many local residual blocks. The global residual connection will force the network to learn the lost information rather than form the signal itself. The local residual blocks make it possible to train deeper network (He et al. 2016). In SRPNet, we use 16 local residual blocks for better performance. The third part is a reconstruction sub-network. In this part, the feature vectors are integrated into  $\alpha$  sub-sequences  $\phi \in \mathbb{R}^{\alpha \times d}$  by two 1D convolution layers. And then rearrange the  $\alpha$  channels of same pixel of the sub-sequences into a new sequence of length  $\alpha$ , corresponding to

an  $\alpha$  size sequence fragment in the high-res data. Thus the  $\alpha$  sub-sequences with length  $d$  is rearranged into the estimated high-res sequence with length  $\alpha \times d$ . This sequence is expected to be similar to the ground truth  $y$ . Different from WaveNet (Van Den Oord et al. 2016) which uses recursive strategy to generate sequence data, we use convolution operation to generate a high-res sequence in parallel. In the rearranging process, upsampling function is implicitly included in the previous convolutional layers and can be learned automatically. This provides higher computational efficiency since convolution operations are performed on low-res sequence size. For WaveNet, it takes about 60 minutes to generate 10000 samples. And it only takes 0.2 seconds for SRPNet to generate a sequence with the same length.

We use mean squared error (MSE) to train our neural network. The loss function is

$$L(y, y') = \|y - y'\|_2^2$$

The network is optimized by minimizing the loss function

$$\theta' = \arg \min_{\theta} L(y, f(x; \theta)) = \arg \min_{\theta} \|y - f(x; \theta)\|_2^2$$

where  $\theta$  is the parameters of neural network  $f$ .

## Discussion

Due to the ill-posedness of the SRP problem, regularization is needed to constrain the solution. In our method, the regularization term is not explicitly included. We next show that our neural network method can be well interpreted under the MAP framework. According to MAP estimation, the corresponding high-res sequence  $y$  given a low-res sequence  $x$  can be estimated by solving following optimization problem

$$y' = \arg \min_y \|\downarrow y - x\|_2^2 + \Omega(y)$$

where  $\|\downarrow y - x\|_2^2$  is the distortion measurement term and  $\Omega(y)$  is the regularization term contains prior information. This equation indicates that  $y'$  is a function of the input  $x$  and degradation function  $\downarrow$ . The MAP solution of SRP problem is equivalent to

$$y' = \mathcal{F}(x, \downarrow; \theta)$$

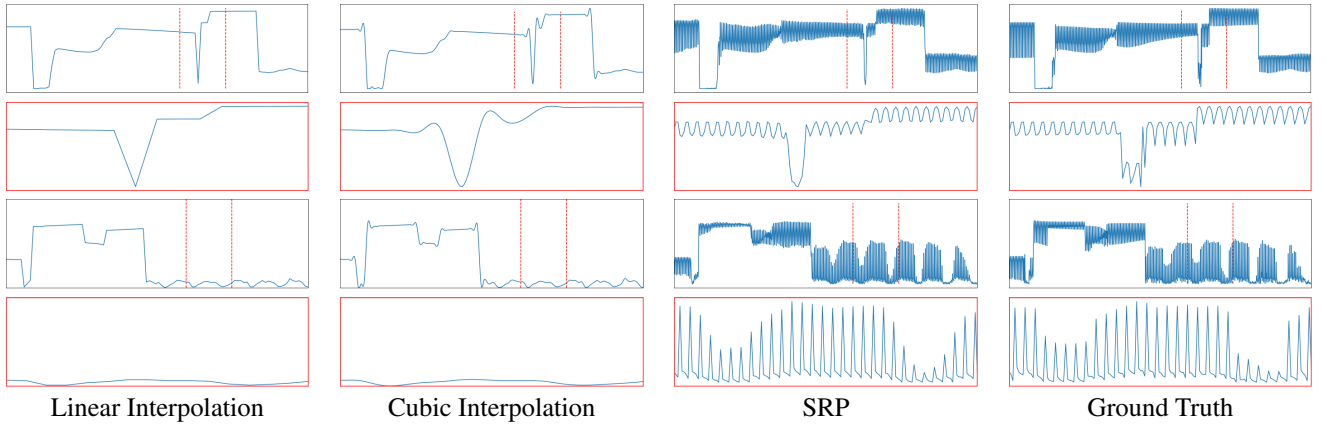


Figure 5: The SRP results of experiment with  $f_l = 10\text{Hz}$  and  $\alpha = 10$ .

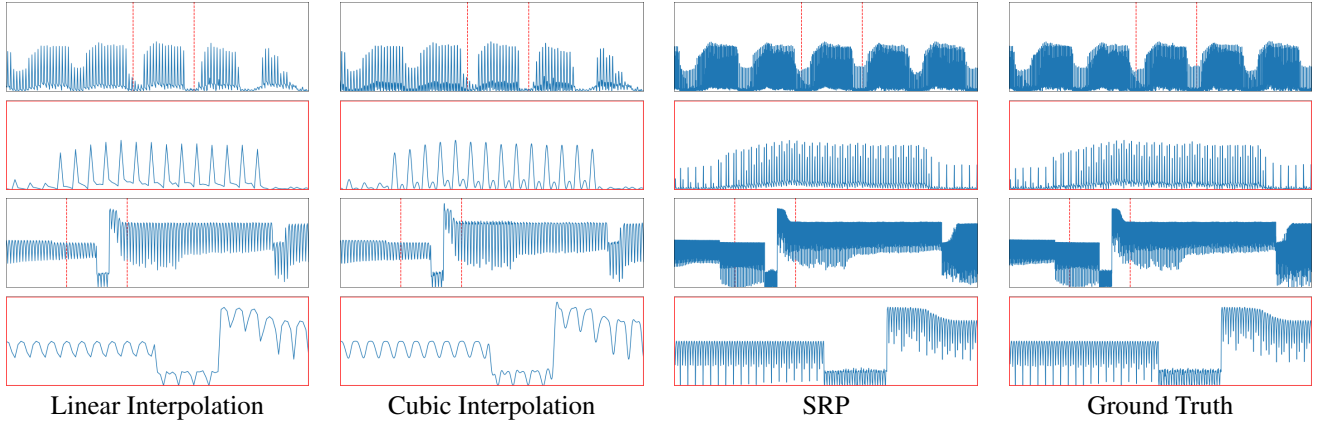


Figure 6: The SRP results of experiment with  $f_l = 100\text{Hz}$  and  $\alpha = 10$ .

When  $\downarrow$  is given, it is equivalent to the SRP mapping  $f$  we proposed above. This equation indicates that actually the prior information is included in the network parameter  $\theta$ . Although we do not modeling the prior of  $h$  explicitly, the neural network trained on a large amount of data contains this prior. The neural network estimates the high-res sequence  $y'$  using a implicit prior knowledge. On the other hand, the proposed neural network not only avoid the direct modeling of the prior of  $y$  but also convert optimization problem into a inference problem, which can improve the calculation efficiency.

## Experiments

In order to study the characteristics and effectiveness of the proposed SRP method, we conducted experiments under three different settings: (1) the low-res data with frequency  $f_l = 10\text{Hz}$  and an SRP factor of  $\alpha = 10$ ; (2)  $f_l = 100\text{Hz}$  and  $\alpha = 10$ ; (3)  $f_l = 10\text{Hz}$  and of  $\alpha = 100$ .

**Data preparation and preprocessing.** We use the simulated smart meter data to train and test the SRPNet. We simulated the working state of electrical appliances in houses and then combine the corresponding electrical load data into a final smart meter data of a house according to the working

state. The used electrical load data of appliance in different states is provided in the Plug-Level Appliance Identification Dataset (PLAID) (De Baets et al. 2017). PLAID can be used in appliance identification, it provides 1793 high resolution (30000Hz) meter data instances of 82 different appliances which belong to 11 different appliance types. Since the electrical load data has a very large dynamic range ( $10^{-3} - 10^6$ ), it is difficult for the neural network to directly process the input and output with a large dynamic range. We preprocess the original large dynamic meter data with following formula

$$\tilde{x} = \log_{100}(x \times 10^3 + 1)$$

This formula is monotonous and ensured  $\tilde{x}$  to be positive. It well preserves the fluctuations in data. The high and low frequency data used for training is based on the degradation model described in the problem formulation section. Since the meter records the instantaneous current and voltage values, we assume the sampled data given high-frequency meter and low-frequency meter are approximately equal. Thus, we employ Nearest Neighbor (NN) down-sampling as the degradation function. Then, a Gaussian noise with a  $\sigma = 0.01$  was added to the down-sampled low-frequency data. In the experiment, we prepare 14000 high frequency data sam-

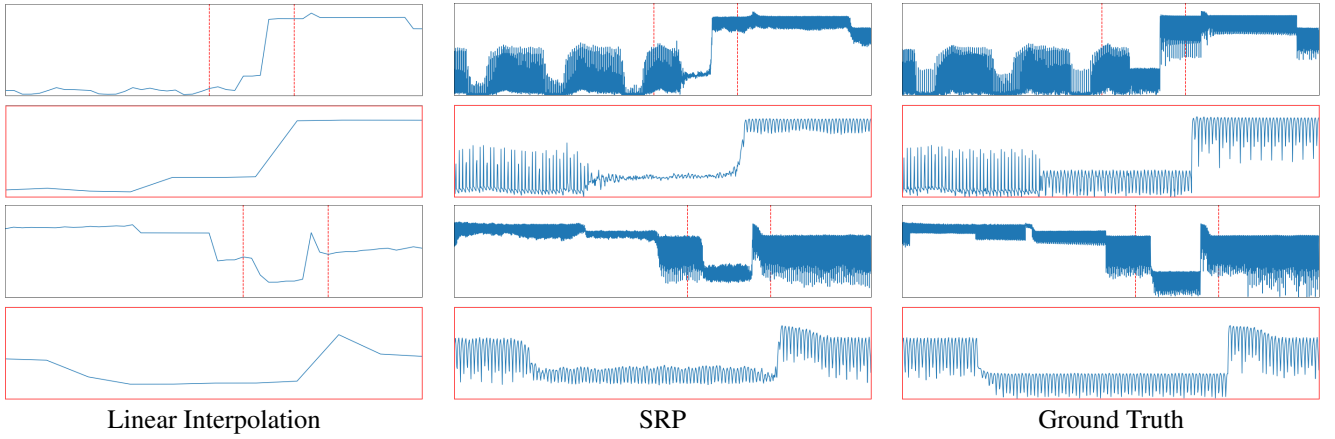


Figure 7: The SRP results of experiment with  $f_l = 10\text{Hz}$  and  $\alpha = 100$ .

Experiment	Linear Interpolation	Cubic Interpolation	SRP
$f_l = 10\text{Hz}, \alpha = 10$	111.9504 / 461.0110	113.9308 / 458.9368	<b>67.2457 / 0.0386</b>
$f_l = 100\text{Hz}, \alpha = 10$	101.7538 / 301.6763	109.1351 / 300.7959	<b>17.5334 / 0.0142</b>
$f_l = 10\text{Hz}, \alpha = 100$	112.8678 / 423.6664	114.7332 / 423.6975	<b>64.0355 / 0.1758</b>

Table 1: The quantitative comparison of different interpolation methods and SRP (RMSE / DTW).

ples of length 30s for training and another 2000 data were used for validation and testing. This dataset will be released.

**Network training.** For optimization, we use Adam (Kingma and Ba 2015) with  $\beta_1 = 0.9$  and  $\beta_2 = 0.999$ . The mini-batch size is set to 32. The learning rate is initialized as  $1 \times 10^{-4}$  for the first  $1 \times 10^6$  mini-batch updates and then fine tuned with learning rate of  $1 \times 10^{-6}$  for another  $1 \times 10^6$  mini-batch updates. We implement our models with the PyTorch framework and train them using NVIDIA Titan Xp GPUs. The entire training process took about twenty hours.

**Result analysis.** Some SRP test results are shown in Figure 5, Figure 6 and Figure 7. The first line of each cases is the overview of a 5 seconds time slice and the second line is the fragment of 1 second marked by red lines in overview for a better view. We compared our SRP results with linear interpolation and cubic interpolation. As can be seen, the interpolation method can not recover the missing details in the high-frequency data due to the loss of information during the degradation process. However, the proposed SRP method restore the waveforms and details effectively. A representative result of SRP is shown in the second case of Figure 5. Its low-frequency data loses most of the information of the waveform, but SRP successfully reconstructs the lost waveform details. To quantify the comparison, we use Root Mean Square Error (RMSE) and Dynamic Time Warping (DTW) (Vintsyuk 1968) as metrics. RMSE is commonly used to measure the temporal similarity of time series and DTW is a well-known technique to find an optimal alignment between two given time series or waveforms. This alignment can be used to measure the spatial similarity between two sequences. DTW is first calculated on the time

window that slides over the time series. The average of all time windows on the time series is the final DTW similarity of the time series. We use a time window with a size equal to 100. The quantitative comparison results are shown in the Table 1. It is obvious that the SRP method is significantly better than the existing interpolation method. We can also find that the experiment of input frequency with 100hz and an SRP factor of 10 has the best SRP result. Because the high-frequency data contains more information on describing the real system state. Thus, it is easy for the generative model to infer the data before degradation. When the frequency of the input data becomes lower, the real system state is more difficult to estimate, and it is more difficult to recover high frequency information therefrom. We can also see that when the SRP factor becomes 100, although the SRP can still recover the high-frequency data to a certain extent, it suffered more severe distortion than the experiment with an SRP factor of 10. These experiments demonstrate that: (1) when the input data has a lower frequency, it is more difficult to perform SRP; (2) it is more difficult to perform SRP with a larger super-resolution factor.

**Nonintrusive load monitoring results.** We then study the application of SRP in Non-Intrusive Load Monitoring (NILM). The main purpose of load monitoring techniques is to reduce energy consumption. NILM is the process of identifying appliances and their working states using a single smart meter. High-frequency data will increase the accuracy of NILM yet requires high-frequency smart meters which are more expensive. We use the SRP results as an alternative of high-frequency data. Three classic NILM algorithms are used for this study: KNN (Berges et al. 2010), SVM (Wu and Chang 2004) and Decision Tree (Rodríguez and Alonso 2004). For every algorithms and experiment settings, mod-



Method	Experiment	trained on LF test on LF	trained on HF test on SRP	trained on HF test on HF	Gain from SRP
KNN	$f_l = 10\text{Hz}, \alpha = 10$	0.5968	0.6006	0.6030	+0.0038
	$f_l = 100\text{Hz}, \alpha = 10$	0.6030	0.6348	0.6993	+0.0318
	$f_l = 10\text{Hz}, \alpha = 100$	0.5968	0.6154	0.6993	+0.0186
Decision Tree	$f_l = 10\text{Hz}, \alpha = 10$	0.6068	0.6328	0.6507	+0.026
	$f_l = 100\text{Hz}, \alpha = 10$	0.6507	0.6849	0.7140	+0.0342
	$f_l = 10\text{Hz}, \alpha = 100$	0.6068	0.6418	0.7140	+0.0350
SVM	$f_l = 10\text{Hz}, \alpha = 10$	0.6705	0.6763	0.6696	+0.0058
	$f_l = 100\text{Hz}, \alpha = 10$	0.6696	0.7199	0.7528	+0.0503
	$f_l = 10\text{Hz}, \alpha = 100$	0.6705	0.7034	0.7528	+0.0329

Table 2: The accuracy results of NILM on different experimental settings. LF denotes low-frequency data and HF denotes high-frequency data.

els are trained on both SRP results and high-frequency data and tested with SRP results. For comparison, the models trained and tested on low-frequency data and high-frequency data are used as baseline. The accuracy results are shown in Table 2, which shows the reconstructed high-frequency data can lead to better appliance monitoring results without changing the monitoring appliances.

## Discussion and Future Work

SRP can be applied into many important industrial fields. State estimation (SE) is one of the most closely related scenarios. SE focuses on estimating system states at a specific time point. SRP will show good performances and play significant roles in aforementioned area.

Industrial state estimation, as an important component of the industrial control process, is mainly performed to estimate system state variables under the state conditions characterized by a set of sensor measurements. Since most of the large-scale industrial systems are deployed decades ago, their state estimations are performed mainly based on low-frequency sampling sensors due to the limitations of sensor and communication technologies. However, the higher standards of modern industry on system efficiency and product quality require more accurate system state estimation. Also, a new source of threats, cyber attackers, are bringing significant challenges to the security of industrial control processes (Liang et al. 2017). For example, Stuxnet targets industrial supervisory control and data acquisition (SCADA) systems and programmable logic controllers (PLC) to cause substantial system damages<sup>1</sup>. Both industrial upgrade and security defense call for more precise monitoring on system running states, while existing low-frequency sampling sensors cannot meet the requirement.

Take the power system state estimation as an example. The power system state estimation is formulated as a non-convex optimization problem, which analyzes measurements of voltage and power at certain nodes to output complete system states (including power, voltage magnitude and angle) (Monticelli 2000). In traditional power system, sensors (low-frequency) were deployed in the remote termi-

nal units (RTUs), and some of the traditional sensors have been replaced by phasor measurement units (PMUs) (high-frequency) recently (London et al. 2009). However, it is impossible to replace all traditional sensors by PMUs because PMU is extremely expensive. Under such circumstances, on the one hand, low-frequency measurements cannot provide high-resolution observations on system states; on the other hand, lots of high-frequency measurements collected from PMUs are wasted, because the industry has no idea how to co-utilize both the high-frequency data collected by a small number of PMUs and the low-frequency data collected by traditional RTUs. This makes power system state estimation a good application of SRP. SRP can supplement enough super-resolution information in between two sets of measurements so as to perceive system states more clearly.

It should be noticed that different from the environment with only a single sensor, state estimation relies on multiple sensors at a specific time point to estimate corresponding state variables, which relies on the domain knowledge of system internal relationships in the space domain (e.g. the relationships between the temperatures of different rooms in a large building). Therefore, both time domain and space domain information may be considered when applying SRP in industrial state estimation, which will be our future work.

## Conclusion

In this paper, we propose a novel machine learning problem - the SRP problem as reconstructing high-quality data from unsatisfactory sensor data in industrial systems. We first mathematically formulate the SRP problem under the Maximum a Posteriori (MAP) estimation framework. Advanced generative models are then proposed to solve the SRP problem on smart meter data. A network namely SRP-Net is proposed to generate high-frequency load data from low-frequency data. Experiments demonstrate that our SRP model can reconstruct high-frequency data effectively and lead to better appliance monitoring results without changing the monitoring appliances.

<sup>1</sup>See <https://en.wikipedia.org/wiki/Stuxnet> for more information.

## References

- [Abramovici, Göbel, and Neges 2015] Abramovici, M.; Göbel, J. C.; and Neges, M. 2015. Smart engineering as enabler for the 4th industrial revolution. In *Integrated systems: Innovations and applications*. Springer. 163–170.
- [Berges et al. 2010] Berges, M. E.; Goldman, E.; Matthews, H. S.; and Soibelman, L. 2010. Enhancing electricity audits in residential buildings with nonintrusive load monitoring. *Journal of industrial ecology* 14(5):844–858.
- [Bretas, Bretas, and Martins 2013] Bretas, N.; Bretas, A.; and Martins, A. C. 2013. Convergence property of the measurement gross error correction in power system state estimation, using geometrical background. *IEEE Transactions on Power Systems* 28(4):3729–3736.
- [De Baets et al. 2017] De Baets, L.; Develder, C.; Dhaene, T.; Deschrijver, D.; Gao, J.; and Berges, M. 2017. Handling imbalance in an extended plaid. In *2017 Sustainable Internet and ICT for Sustainability (SustainIT)*, 1–5. IEEE.
- [Dong et al. 2016] Dong, C.; Loy, C. C.; He, K.; and Tang, X. 2016. Image super-resolution using deep convolutional networks. *IEEE transactions on pattern analysis and machine intelligence* 38(2):295–307.
- [Gao, Cecati, and Ding 2015] Gao, Z.; Cecati, C.; and Ding, S. X. 2015. A survey of fault diagnosis and fault-tolerant techniquespart i: Fault diagnosis with model-based and signal-based approaches. *IEEE Transactions on Industrial Electronics* 62(6):3757–3767.
- [Goodfellow et al. 2014] Goodfellow, I.; Pouget-Abadie, J.; Mirza, M.; Xu, B.; Warde-Farley, D.; Ozair, S.; Courville, A.; and Bengio, Y. 2014. Generative adversarial nets. In *Advances in neural information processing systems*, 2672–2680.
- [He et al. 2016] He, K.; Zhang, X.; Ren, S.; and Sun, J. 2016. Deep residual learning for image recognition. In *Proceedings of the IEEE conference on computer vision and pattern recognition*, 770–778.
- [Kim, Lee, and Lee 2016] Kim, J.; Lee, J. K.; and Lee, K. M. 2016. Accurate image super-resolution using very deep convolutional networks. In *Computer Vision and Pattern Recognition (CVPR), 2016 IEEE Conference on*, 1646–1654. IEEE.
- [Kingma and Ba 2015] Kingma, D. P., and Ba, J. 2015. Adam: A method for stochastic optimization. In *ICLR*.
- [Kingma and Welling 2014] Kingma, D. P., and Welling, M. 2014. Auto-encoding variational bayes. In *Proceedings of the International Conference on Learning Representations (ICLR)*.
- [Kriaa et al. 2015] Kriaa, S.; Pietre-Cambacedes, L.; Bouissou, M.; and Halgand, Y. 2015. A survey of approaches combining safety and security for industrial control systems. *Reliability Engineering & System Safety* 139:156–178.
- [Kupyn et al. 2017] Kupyn, O.; Budzan, V.; Mykhailych, M.; Mishkin, D.; and Matas, J. 2017. Deblurgan: Blind motion deblurring using conditional adversarial networks. *ArXiv e-prints*.
- [Lasi et al. 2014] Lasi, H.; Fettke, P.; Kemper, H.-G.; Feld, T.; and Hoffmann, M. 2014. Industry 4.0. *Business & Information Systems Engineering* 6(4):239–242.
- [Liang et al. 2017] Liang, G.; Zhao, J.; Luo, F.; Weller, S. R.; and Dong, Z. Y. 2017. A review of false data injection attacks against modern power systems. *IEEE Transactions on Smart Grid* 8(4):1630–1638.
- [Lim et al. 2017] Lim, B.; Son, S.; Kim, H.; Nah, S.; and Lee, K. M. 2017. Enhanced deep residual networks for single image super-resolution. In *The IEEE conference on computer vision and pattern recognition (CVPR) workshops*, volume 1, 4.
- [London et al. 2009] London, J.; Piereti, S. A. R.; Benedito, R.; and Bretas, N. 2009. Redundancy and observability analysis of conventional and pmu measurements. *IEEE Transactions on Power Systems* 24(3):1629–1630.
- [Mao, Shen, and Yang 2016] Mao, X.; Shen, C.; and Yang, Y.-B. 2016. Image restoration using very deep convolutional encoder-decoder networks with symmetric skip connections. In Lee, D. D.; Sugiyama, M.; Luxburg, U. V.; Guyon, I.; and Garnett, R., eds., *Advances in Neural Information Processing Systems* 29. Curran Associates, Inc. 2802–2810.
- [Monticelli 2000] Monticelli, A. 2000. Electric power system state estimation. *Proceedings of the IEEE* 88(2):262–282.
- [Qin 2012] Qin, S. J. 2012. Survey on data-driven industrial process monitoring and diagnosis. *Annual reviews in control* 36(2):220–234.
- [Rezende, Mohamed, and Wierstra 2014] Rezende, D. J.; Mohamed, S.; and Wierstra, D. 2014. Stochastic back-propagation and approximate inference in deep generative models. *arXiv preprint arXiv:1401.4082*.
- [Rodríguez and Alonso 2004] Rodríguez, J. J., and Alonso, C. J. 2004. Interval and dynamic time warping-based decision trees. In *Proceedings of the 2004 ACM symposium on Applied computing*, 548–552. ACM.
- [Van Den Oord et al. 2016] Van Den Oord, A.; Dieleman, S.; Zen, H.; Simonyan, K.; Vinyals, O.; Graves, A.; Kalchbrenner, N.; Senior, A. W.; and Kavukcuoglu, K. 2016. Wavenet: A generative model for raw audio. In *SSW*, 125.
- [Vintsyuk 1968] Vintsyuk, T. K. 1968. Speech discrimination by dynamic programming. *Cybernetics* 4(1):52–57.
- [Wu and Chang 2004] Wu, Y., and Chang, E. Y. 2004. Distance-function design and fusion for sequence data. In *Proceedings of the thirteenth ACM international conference on Information and knowledge management*, 324–333. ACM.
- [Yeh et al. 2017] Yeh, R. A.; Chen, C.; Lim, T.-Y.; Schwing, A. G.; Hasegawa-Johnson, M.; and Do, M. N. 2017. Semantic image inpainting with deep generative models. In *CVPR*, volume 2, 4.
- [Zhang et al. 2017a] Zhang, J.; Pan, J.; Lai, W.-S.; Rynson, W.; and Yang, M.-H. 2017a. Learning neural networks for iterative non-blind deconvolution. In *IEEE CVPR 2017*.



[Zhang et al. 2017b] Zhang, K.; Zuo, W.; Chen, Y.; Meng, D.; and Zhang, L. 2017b. Beyond a gaussian denoiser: Residual learning of deep cnn for image denoising. *IEEE Transactions on Image Processing* 26(7):3142–3155.